

Ruby, metals, and MgO as alternative pressure scales: A semiempirical description of shock-wave, ultrasonic, x-ray, and thermochemical data at high temperatures and pressures

Peter I. Dorogokupets^{1,*} and Artem R. Oganov^{2,3,†}

¹*Institute of the Earth's Crust SB RAS, Irkutsk 664033 Russia*

²*Laboratory of Crystallography, ETH Zurich, CH-8093 Zurich, Switzerland*

³*Geology Department, Moscow State University, Moscow 119899, Russia*

(Received 6 May 2006; published 25 January 2007)

We have constructed semiempirical equations of state of Al, Au, Cu, Pt, Ta, and W, which within experimental error bars describe the available shock-wave, ultrasonic, x-ray, and thermochemical data in the temperature range from 10–20 K up to the melting temperature and to compression $x=V/V_0=0.5-0.7$. The comparison of the calculated room-temperature isotherms for these metals with quasihydrostatic measurements supports recently proposed ruby pressure scales. We recommend a new ruby pressure scale in the form $P=A(\Delta\lambda/\lambda_0)\times(1+m\Delta\lambda/\lambda_0)$ with parameters $A=1884$ GPa and $m=5.5$. The cross check on independent data confirms the obtained *PVT* equations of state of Ag, Al, Au, Cu, Pt, Ta, W, MgO, and diamond. The equations of state of these materials obtained here provide accurate and versatile means for calibrating pressure at all temperatures below the melting point. Furthermore, they can be used for accurate tabulation of thermodynamic properties (heat capacities, entropies) of these reference substances in a wide P-T range.

DOI: 10.1103/PhysRevB.75.024115

PACS number(s): 64.30.+t, 05.70.Ce, 65.40.-b

I. INTRODUCTION

More than a decade after the invention of diamond anvil cell (DAC) (Ref. 1), in the beginning of 1970s, the optical ruby fluorescence method of pressure measurement was developed.² With the efforts of many researchers²⁻⁶ in 1970s and 1980s the ruby pressure scale was calibrated up to megabar pressures and became the *de facto* standard for pressure measurements in the DAC in the end of the twentieth and beginning of the twenty-first centuries (see reviews in Refs. 7-9).

With the ruby pressure scale, pressure is obtained from the R_1 line shift of ruby luminescence. This is a secondary pressure scale, requiring a careful calibration. The most popular calibration due to Mao *et al.*⁶ is based on the measurements of the R_1 line shift of ruby luminescence in the Ar pressure medium up to a pressure of 80 GPa. The pressure was determined from the room-temperature isotherms of Cu and Ag reduced by Carter *et al.*¹⁰ from shock-wave data. The value for the initial slope of $P(\lambda)$, $A=\lambda(dP/d\lambda)=1904$ GPa, has been obtained by Piermarini *et al.*³ with the use of Decker's¹¹ equation of state (EOS) of NaCl as pressure standard in the quasihydrostatic medium (up to 10.4 GPa) and in the nonhydrostatic medium up to the pressure of 19.5 GPa. The resulting pressure scale of Mao *et al.*⁶ is expressed as

$$P = \frac{A}{B}[(1 + \Delta\lambda/\lambda_0)^B - 1],$$

$$P = \frac{A}{B}[(\lambda/\lambda_0)^B - 1], \quad (1a)$$

where P is pressure in GPa, $A=\lambda(\partial P/\partial\lambda)=1904$ GPa, $B=7.665$, $\lambda_0=694.24$ nm.

Almost at the same time, Aleksandrov *et al.*¹² published a significantly different calibration of the ruby scale based on the *a priori* EOS of diamond. Aleksandrov *et al.*¹² performed simultaneous measurements of the R_1 line shift of ruby luminescence and spectra of the first-order Raman light scat-

tering of diamond in a DAC with helium pressure-transmitting medium up to the compression of $x=V/V_0=0.93$. Trying various pressure scales, Aleksandrov *et al.*¹² obtained unrealistically low values of the pressure derivatives of the bulk modulus ($K'=dK/dP$) for diamond: 1, 1.9, and 2.5 for scales from Refs. 3, 5, and 8, respectively, in conflict with theory,^{13,14} and ultrasonic measurements.¹⁵ Assuming a much more realistic value of $K'=4$ for diamond, Aleksandrov *et al.*¹² arrived at a new pressure scale with parameters $A=1918$ GPa and $B=11.7$ for Eq. (1). Aleksandrov *et al.*¹² also proposed another form for the pressure scale:

$$P = A(\Delta\lambda/\lambda_0)(1 + m\Delta\lambda/\lambda_0) \quad (2)$$

with parameters $A=1892\pm 13$ GPa and $m=6.4$. This scale begins to differ from the scale of Ref. 6 above 20 GPa, and leads to significant differences at pressures greater than 50 GPa (Fig. 1).

Hemley *et al.*¹⁶ have obtained the EOS of solid neon up to 110 GPa using the ruby⁶ and tungsten¹⁷ pressure scales and have overall confirmed the ruby scale of Mao *et al.*⁶ However, they noticed that pressures from the tungsten scale are systematically higher (5%) than those from the ruby scale at high compression, but this difference was within the expected error in the tungsten isotherm (Ref. 16, p. 11822). Helium remains considerably weaker than neon and argon at high pressure,¹⁸ therefore Hemley *et al.*¹⁶ suggested that part of the differences between the ruby scales of Aleksandrov *et al.*¹² and Mao *et al.*⁶ may be associated with residual nonhydrostatic effects in the Ar pressure medium used in Ref. 6.

Recently, Zha *et al.*¹⁹ measured the elastic constants of MgO up to a pressure of 55 GPa using Brillouin scattering. By combining the Brillouin and x-ray measurements, they obtained the equation of MgO state and calculated a new ruby scale in the form (1) with $A=1904$ GPa and $B=7.715$, close to the calibration of Mao *et al.*⁶

However, a series of works²⁰⁻²⁴ were recently published, in which the ruby pressure scale of Mao *et al.*⁶ has been

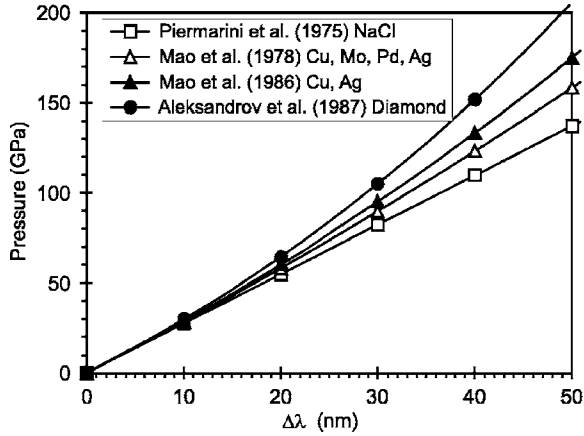


FIG. 1. Comparison of early calibrations of the ruby pressure scale. The linear relation comes from Piermarini *et al.* (Ref. 3). The nonlinear functions were calculated with Eq. (1): $A=1904$ GPa and $B=5$ (Mao *et al.* (Ref. 5), nonhydrostatic conditions), $A=1904$ GPa and $B=7.665$ (Mao *et al.* (Ref. 6), quasihydrostatic conditions, argon pressure transmitting medium), $A=1918$ GPa and $B=11.5$ (Aleksandrov *et al.* (Ref. 12) quasihydrostatic conditions, helium pressure transmitting medium).

considerably shifted toward the scale of Aleksandrov *et al.*¹²

The scale of Holzapfel²⁰ is based on a comparison of recent high-pressure x-ray diffraction data for diamond and Ta with low-pressure ultrasonic data. It shows a significant difference from the scales of Mao *et al.*^{5,6} and comes close to the scale of Aleksandrov *et al.*¹² It has the following form:

$$P = \frac{A}{B+C} \left[\exp\left(\frac{B+C}{C} [1 - (\lambda/\lambda_0)^{-C}]\right) - 1 \right], \quad (3)$$

where $A=1820$ GPa, $B=14$, $C=7.3$, and corresponds to Eq. (1) in the limit of $C \rightarrow 0$.

Dorogokupets and Oganov²¹ have constructed the EOSs of Cu and Ag, which agree with experimental measurements in the temperature range from 10–20 K up to the melting temperature and up to the compression $x=0.6$, and have obtained a ruby pressure scale with parameters $A=1871$ GPa and $B=10.06$ for Eq. (1). This scale agrees quite well with the Holzapfel scale²⁰ up to 100 GPa.

Kunc *et al.*^{22,23} have compared the theoretical EOS of diamond with high-quality data of Ocelli *et al.*²⁵ on x-ray diffraction of diamond in DAC with helium pressure-transmitting medium. Using the ruby scale of Mao *et al.*,⁶ Ocelli *et al.*²⁵ obtained the value $K'=3.0 \pm 0.1$, and this value appeared too low in comparison with the value from ultrasonic measurements $K'=4 \pm 0.5$ (Ref. 15) and theoretical value $K'=3.65 \pm 0.05$ of Kunc *et al.*^{22,23} Kunc *et al.*^{22,23} have assumed that the discrepancy between experimental and calculated EOS and phonon frequencies of diamond is caused by some error in the Mao *et al.*⁶ ruby pressure scale. To remove the discrepancy for the phonon frequency, Kunc *et al.*^{22,23} have proposed a revised ruby scale in the form

$$P = A(\Delta\lambda/\lambda)(1 + \mu\Delta\lambda/\lambda) \quad (4)$$

with parameters $A=1860$ GPa and $\mu=7.75$.

For calibration of the ruby pressure scale, it is necessary to recognize as revolutionary the work of Dewaele *et al.*,^{24,26} where PV relations at room temperature have been measured for Ta, Au, and Pt to 94 GPa and for Al, Cu, and W to 153 GPa in DAC with helium pressure-transmitting medium. When they compared the EOSs of these metals based on the ruby scale of Mao *et al.*⁶ and the room-temperature isotherms obtained by reducing shock-wave data^{27–29} it appeared that they differ by up to 8–9 GPa at pressures of 100–150 GPa. Correcting the ruby pressure scale for these differences, Dewaele *et al.*²⁴ have obtained a new pressure scale with parameters $A=1904$ GPa and $B=9.5$ for Eq. (1). This scale gives practically the same pressures as scales of Holzapfel²⁰ and of Dorogokupets and Oganov.²¹

Here we present a general thermodynamic formalism, using which we construct semiempirical EOSs of several reference substances (Ag, Al, Au, Cu, Pt, Ta, W, diamond, MgO) in the temperature range 10–15 K to the melting temperature and up to pressures 200–300 GPa (compression $x = V/V_0 = 0.5–0.7$). We show that these EOSs accurately describe experimental measurements of the heat capacity, thermal expansion, and adiabatic bulk modulus at 1 atm and the data from the Shock Wave Database [SWDB (Ref. 30)]. Comparison of our calculated room-temperature isotherms with quasihydrostatic data of Dewaele *et al.*^{24,26} allowed us to obtain a new ruby pressure scale. Based on the newly obtained ruby pressure scale, we explored different functional forms for $P(\lambda)$, and found that the form (1) is valid for pressures below 100 GPa. Cross checks between the obtained EOSs of Ag, Al, Au, Cu, Pt, Ta, W, MgO and independent data further validate our results and show that the obtained EOSs of all studied substances are consistent with each other on different isotherms and with the ruby pressure scale on room isotherm. As a basis of construction of the EOS we will use the expanded formalism from Ref. 21.

II. THERMODYNAMICS

Let us write the Helmholtz free energy $F(V, T)$ as the sum³¹

$$F = U_0 + E(V) + F_{\text{qh}}(V, T) + F_{\text{anh}}(V, T) + F_{\text{el}}(V, T) + F_{\text{def}}(V, T), \quad (5)$$

where U_0 is the reference energy, $E(V)$ is the potential (cold) part of the free energy on the reference isotherm, which depends only on volume; $F_{\text{qh}}(V, T)$, $F_{\text{anh}}(V, T)$, $F_{\text{el}}(V, T)$, and $F_{\text{def}}(V, T)$ are the quasiharmonic part of the Helmholtz free energy, and terms describing intrinsic anharmonicity, electronic contribution, and thermal defects.

Differentiating (5), we obtain all the necessary thermodynamic functions: entropy, $S = -(\partial F / \partial T)_V$, internal energy $E = F + TS$, heat capacity at constant volume, $C_V = (\partial E / \partial T)_V$, pressure, $P = -(\partial F / \partial V)_T$, isothermal bulk modulus, $K_T = -V(\partial P / \partial V)_T$, slope of pressure at constant volume $(\partial P / \partial T)_V = \alpha K_T$, where $\alpha = 1/V(\partial V / \partial T)_P$. Heat capacity at constant pressure is $C_P = C_V + \alpha^2 TVK_T$, adiabatic bulk modulus is $K_S = K_T + VT(\alpha K_T)^2 / C_V$. The enthalpy and Gibbs energy can be found from $H = E + PV$, $G = F + PV$.

Cold energy, pressure, and bulk modulus are written as³²

$$E(V) = 9K_0V_0\eta^{-2}\{1 - [1 - \eta(1 - y)]\exp[(1 - y)\eta]\}, \quad (6)$$

$$P(V) = -\partial E/\partial V = 3K_0y^{-2}(1 - y)\exp[(1 - y)\eta], \quad (6a)$$

$$K(V) = K_0y^{-2}[1 + (\eta y + 1)(1 - y)]\exp[(1 - y)\eta], \quad (6b)$$

where $y = x^{1/3} = (V/V_0)^{1/3}$ and $\eta = 1.5(K' - 1)$, $K' = dK/dP$, V_0 , and K_0 are molar volume and bulk modulus at reference conditions ($T_0 = 298.15$ K, $P_0 = 1$ bar).

For approximation of the quasiharmonic phonon part of the Helmholtz free energy through the whole range of temperatures we use a modified formalism of Kut'in *et al.*^{33,34}

$$F_{\text{qh}} = m_B R \left[\frac{(d-1)}{2d} \Theta_B - T \ln(1+b) \right], \quad (7)$$

where R is the gas constant, m_B is the number of phonon modes; $b = 1/[\exp(g) - 1]$, $g = d \ln[1 + \Theta_B/(Td)]$, d is the exponential parameter controlling the behavior of the low-temperature limiting behavior of the heat capacity, and Θ_B is the characteristic temperature. These authors noticed that this analytical function yields both a $C_V \sim T^d$ dependence of the heat capacity at low temperatures and constant limit $C_V = m_B R$ at high temperatures. Kut'in *et al.*^{33,34} have shown that Eq. (7) in combination with the Einstein function approximates well thermodynamic functions from 0 K up to the ambient temperature and higher. This formalism can be used for analytical representation of the quasiharmonic part of the Helmholtz free energy, which can be written as

$$F_{\text{qh}} = \sum_i m_{B_i} R \left[\frac{(d_i-1)}{2d_i} \Theta_{B_i} - T \ln(1+b_i) \right] + \sum_j m_{E_j} R \left[\frac{\Theta_{E_j}}{2} + T \ln \left(1 - \exp \frac{-\Theta_{E_j}}{T} \right) \right], \quad (8)$$

where Θ_{B_i} and Θ_{E_j} are the Bose-Einstein and the Einstein characteristic temperatures, which depend on volume (or $x = V/V_0$). Usually for a very accurate approximation it is enough to take two Bose-Einstein contributions and two Einstein contributions.

For the volume dependence of the Grüneisen parameter we used the Al'tshuler *et al.*³⁵ form:

$$\gamma = \gamma_\infty + (\gamma_0 - \gamma_\infty)(V/V_0)^\beta = \gamma_\infty + (\gamma_0 - \gamma_\infty)x^\beta, \quad (9)$$

where γ_0 is the Grüneisen parameter at ambient conditions, γ_∞ is the Grüneisen parameter at infinite compression ($x = 0$), and β is a fitted parameter. The form (9) is simple and convenient, has a correct behavior at infinite compression ($\gamma \rightarrow \text{constant}$, $q \rightarrow 0$) and in our experience describes extremely well results of theoretical calculations. From (9) it is possible to calculate the volume dependence of each characteristic temperature (here we use the same γ for all frequencies) and parameter q :

$$\Theta = \Theta_0 x^{-\gamma_\infty} \exp \left[\frac{\gamma_0 - \gamma_\infty}{\beta} (1 - x^\beta) \right], \quad (10)$$

$$q = d \ln \gamma / d \ln V = \beta x^\beta \frac{\gamma_0 - \gamma_\infty}{\gamma}. \quad (11)$$

We describe the contribution of intrinsic anharmonicity to the Helmholtz free energy using the formulation of Oganov and Dorogokupets:³⁶

$$F_{\text{anh}} = \sum_{i,j} m_{i,j} R \frac{ax^m}{6} \times \left[\left(\frac{1}{2} \Theta_{i,j} + \frac{\Theta_{i,j}}{e^{\Theta_{i,j}/T} - 1} \right)^2 + 2 \left(\frac{\Theta_{i,j}}{T} \right)^2 \frac{e^{\Theta_{i,j}/T}}{(e^{\Theta_{i,j}/T} - 1)^2} \times T^2 \right], \quad (12)$$

where indices i and j denote Bose-Einstein and Einstein terms, respectively. Equation (12) was obtained in the first order of thermodynamic perturbation theory and has correct high- and low-temperature behavior, and contains a contribution of zero-point anharmonic effects.

The electronic component of the Helmholtz free energy is taken as

$$F_{\text{el}} = -\frac{3}{2} n R e x^g T^2, \quad (13)$$

where we assume the free-electron value $g = 2/3$ for Cu, Ag, and Au.³¹

For the contribution of thermal defects we use the commonly accepted approximation of independent monovacancies:³⁷

$$F_{\text{def}} = -\frac{3}{2} n R T \exp \left(S x^f - \frac{H x^h}{T} \right), \quad (14)$$

where S and H are the entropy and enthalpy of formation of a monovacancy, respectively, and for all metals we assumed $f = -1$, $h = -2$.

Pressure on the shock-wave adiabat was calculated as follows:³¹

$$P_H = \frac{P(V) - \frac{\gamma}{V} [E(V) - E_0]}{1 - \frac{\gamma(1-x)}{2x}}. \quad (15)$$

Our procedure for finding the parameters describing thermodynamics and EOSs consists of two stages. In the first stage, we find preliminary values of the parameters using weighted least-squares fitting to experimental data unbiased by pressure calibration (i.e., measurements at 1 atm and shock-wave data). It starts with some reasonable guesses for V_0 , K_0 , K' , and γ_0 . Low-temperature measurements of the heat capacity (up to 300–350 K) lead to the determination of the characteristic temperatures (Θ_{B1} , Θ_{B2} , Θ_{E1} , Θ_{E2}) and d_1 , d_2 , m_{B1} , m_{B2} , m_{E1} , m_{E2} parameters (with the constraint that the total number of modes m_{B_i} and m_{E_j} must be equal $3n$, where n is the number of atoms). The starting value of the anharmonicity parameter a is estimated from high-temperature measurements of the heat capacity or relative enthalpy. With this starting set of parameters, we optimize all the parameters by simultaneous fitting of the available experimental data on the heat capacity and relative enthalpy, volume, thermal expansion, and adiabatic bulk modulus at zero pressure and various temperatures, and Hugoniot pressure at x . The full solution allowed us to find all the necessary parameters: V_0 , K_0 , K' , Θ_{B1} , Θ_{B2} , Θ_{E1} , Θ_{E2} , d_1 , d_2 , m_{B1} ,

m_{B2} , m_{E1} , m_{E2} , γ_0 , γ_∞ , β , a , m , e , H , S . Some of these parameters, however, could in principle be specified *a priori*, e.g., from accurate theoretical calculations or from other sources. For example, from the measurements of the heat capacity up to 30 K it is possible to estimate the electronic contribution to the heat capacities [parameter e in Eq. (13)]. Fitted values of e (Table I) do not exceed the values obtained from the experimental measurements of heat capacity. For the contribution of thermal defects, parameters f and h determining volumetric dependence of the defect enthalpy and entropy were fixed. The contribution of thermal defects to the Helmholtz free energy can be estimated also from various experimental data (see, for example, Ref. 38).

In the second stage we also include static compression data calibrated with different pressure scales, refit all the parameters and check their consistency with ultrasound measurements of K_S as a function of temperature at 1 atm. With the above formulation we can carry out a simultaneous processing of all the available measurements of the heat capacity, thermal expansion coefficient, volume, and adiabatic and isothermal bulk moduli at zero pressure, static measurements of volume on a room-temperature isotherm and at higher temperatures, shock-wave data, and calculate any thermodynamic functions vs T and V or vs T and P . In practical realization, we write the Helmholtz free energy relative to the reference conditions $T_0=298.15$ K and $P_0=1$ bar; consequently, the fitted parameters that we find correspond to ambient conditions. At those conditions it is usually easy to verify our parameters by performing direct measurements.

III. RESULTS

First, we obtained all the fitted parameters from a simultaneous processing of experimental data for C_p , α , V , K_S at zero pressure and shock-wave data. Originally such analysis has been carried out for Al, Cu, Ta, and W, for which the values of K_0 and K' equal to 73.46 GPa and 4.52, 133.98 GPa and 5.41, 191.44 GPa and 3.93, 306.23 GPa and 4.16 at ambient conditions have been obtained, and this results in a catastrophic divergence from the data of Dewaele *et al.*²⁴ above 30 GPa if the Mao *et al.*⁶ ruby pressure scale is used for calibrating pressure for experimental data of Dewaele *et al.*²⁴— see Fig. 2(a).

From the EOSs of these metals a preliminary ruby scale with parameters $A=1885$ GPa and $B=10.4$ for Eq. (1) was obtained. Parameter A has been fixed as the average of Piermarini *et al.*³ data for quasihydrostatic conditions ($A=1896$ GPa, also used in Ref. 21) and direct determination $A=1875\pm 30$ GPa.³⁹ Nakano *et al.*⁴⁰ at 10 K and pressures 0–22 GPa found $dP/d\lambda=2.748\pm 0.012$ GPa/nm, from which $A=1908\pm 8$ GPa, close to the result of Ref. 3. However, Holzapfel²⁰ and Syassen⁴¹ commented that the initial slope $dP/d\lambda$ should be smaller than the results of Refs. 3 and 40.

Using this pressure scale for calibration of the Dewaele *et al.*²⁴ measurements, the EOSs for Au and Pt have been obtained. The differences from Dewaele *et al.*²⁴ pressure calculated using the ruby pressure scale with parameters $A=1885$ GPa and $B=10.4$ for Eq. (1) are shown in Fig. 2(b).

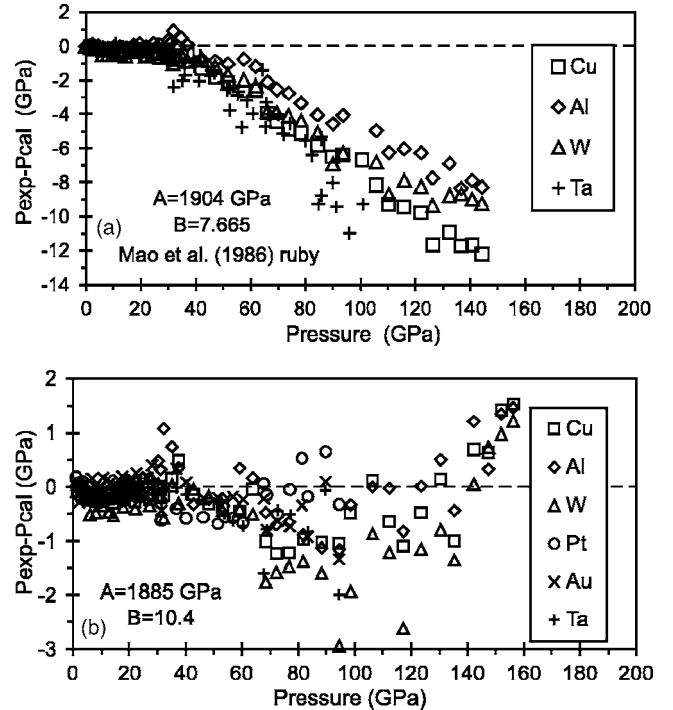


FIG. 2. (a) Pressure difference for the Dewaele *et al.* (Refs. 24 and 26) measurements calibrated using the Mao *et al.* (Ref. 6) ruby scale and our calculated room-temperature isotherms for Cu, Al, Ta, and W. (b) Difference between the Dewaele *et al.* (Refs. 24 and 26) pressure using the ruby scale with parameters $A=1885$ GPa and $B=10.4$ for Eq. (1) and our calculated room-temperature isotherms for Cu, Al, Ta, Pt, Au, and W.

Though the differences are small (within 2 GPa, i.e., 2–3%), Fig. 2(b) shows a minimum of absolute deviations in the pressure range 70–120 GPa. If one assumes that the experimental measurements of Dewaele *et al.*²⁴ are absolutely reliable, then it is necessary to continue the analysis.

We consider two possible causes of this minimum:

- (1) phase transitions of ruby at these pressures;⁴²
- (2) functional dependence (1) is not suitable for high-pressure extrapolation.

We have carried out an additional analysis of the EOSs of all six metals studied in Ref. 24 up to 100 GPa (fitted parameters are listed in Table I), varying parameter B in Eq. (1) and recalculating all the EOSs until consistency with all the experimental measurements of thermodynamic functions at zero pressure (C_p , α , K_S) and measurements of pressure at given volume.

As a result we have obtained a new ruby pressure scale with parameters $A=1885$ GPa and $B=11$ for Eq. (1), which agrees very well with the data of Dewaele *et al.*²⁴ up to the pressure of 100 GPa (Fig. 3). However, above 100 GPa we have systematic deviations from the measurements of Dewaele *et al.*²⁴ If this is due to a phase transition, then we need two ruby pressure scales: one with $A=1885$ GPa and $B=11$ for Eq. (1) up to the pressure 85 GPa, the other with $A=1975$ GPa and $B=8.59$ at pressures above 85 GPa. However, it is likely that at room temperature ruby will keep its structure in the metastable state even at ultrahigh pressures,

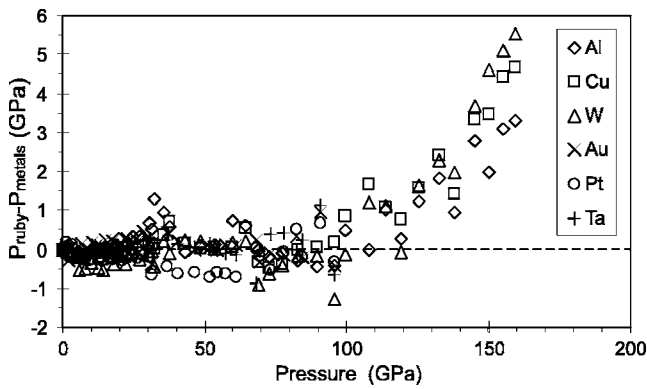


FIG. 3. Difference between the Dewaele *et al.* (Refs. 24 and 26) pressure using the ruby scale with parameters $A=1885$ GPa and $B=11$ for Eq. (1) and our calculated room-temperature isotherms for Cu, Al, Ta, Pt, Au and W. From here on we show pressures according to our present scale (16).

and thus a search for an alternative functional form is needed for the ruby pressure scale.

Among alternative $P(\lambda)$ functional forms, one could use the Holzapfel²⁰ three-parametrical equation in the form (3), however, we find that better results are obtained with the two-parametrical equation in the Aleksandrov *et al.*¹² form:

$$P = 1884 \times (\Delta\lambda/\lambda_0) \times (1 + 5.5\Delta\lambda/\lambda_0). \quad (16)$$

Now the deviations of the calculated room-temperature isotherms from the data of Dewaele *et al.*^{24,26} are very small, only occasionally slightly in excess of 1 GPa at pressures up to 160 GPa (Fig. 4). Figure 5 shows recent calibrations of the ruby pressure scale in comparison with previous calibrations of Mao *et al.*⁶ and Aleksandrov *et al.*¹² and recalculated data of Dewaele *et al.*^{24,26} for Al, Cu, and W using the ruby pressure scale in the form (16), at pressures in the range 100–155 GPa.

As just described, we have obtained two variants of the ruby pressure scale with different functional dependences $P(\lambda)$ which give identical pressure up to 155 GPa. As the final version we prefer Eq. (16) which has the form proposed by Aleksandrov *et al.*¹² The final parameters of the EOSs of the reference materials considered here are given in Table I.

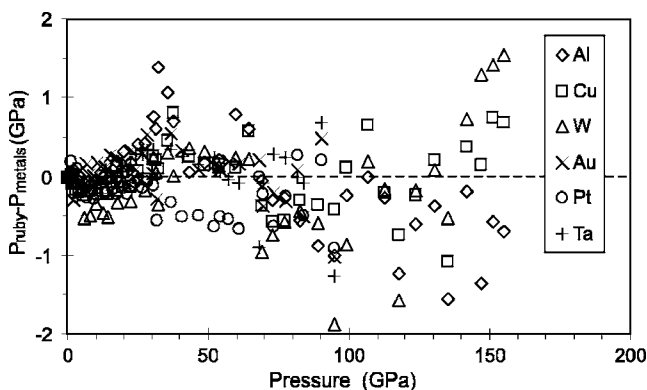


FIG. 4. Difference between the Dewaele *et al.* (Refs. 24 and 26) pressure using the ruby pressure scale (16) and our calculated room-temperature isotherms for Cu, Al, Ta, Pt, Au, and W.

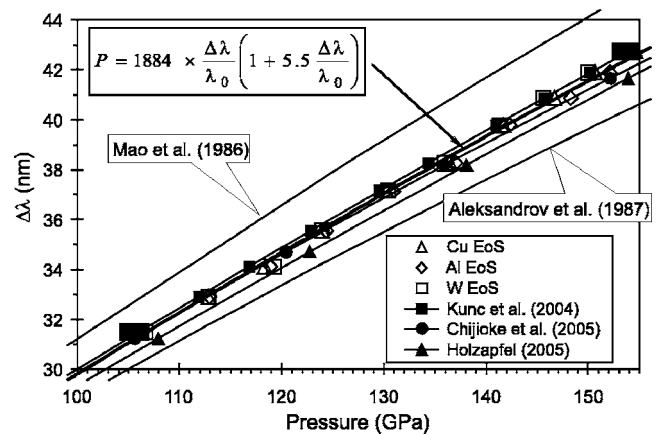


FIG. 5. Comparison of recent ruby pressure scales [Kunc *et al.* (Refs. 22, 23, and 41) Chijioke *et al.* (Ref. 43), Holzapfel, (Ref. 44) and Eq. (16)] at pressures 100–155 GPa with previous calibrations of Mao *et al.* (Ref. 6) and Aleksandrov *et al.* (Ref. 12). Black rectangles are pressures calculated using the ruby scales of Refs. 20, 21, and 24 (they nearly coincide on the scale of this figure). Also shown are pressures calibrated from the EOSs of Cu, Al, and W obtained here.

We conclude that the EOSs of Al, Au, Cu, Pt, Ta, and W obtained here agree with experimental measurements in the temperature and pressure ranges considered here with an error comparable to that of direct measurements (comparison of the calculated and experimental thermodynamic functions is shown in Fig. 6 for the case of tungsten and in Dorogokupets and Oganov⁴⁵ for the case of gold). One can expect that the obtained EOSs will be also correct at higher temperatures and pressures, which will be confirmed through the comparison of the EOSs of gold, platinum, silver, and MgO.

A critical role in our approach is played by the ultrasonic measurements of the temperature dependence of the adiabatic bulk modulus in a wide range of temperatures at zero pressure. Comparison of these data with our calculation is shown on Fig. 7, which shows good agreement of our calculation with ultrasonic data.

Figure 7 shows the adiabatic bulk modulus of Au calculated by Shim *et al.*,⁷³ which differs significantly from experiment and our calculation. The main cause of this discrepancy is the value $K'=5$ recommended in Ref. 73 for gold ($K'=5$ comes from Ref. 89, where the pressure scale of Zha *et al.*¹⁹ was used), which is significantly lower than results of Table I and Ref. 66. The second reason is that the Mie-Grüneisen formalism, used in Ref. 73 and valid in the framework of the quasiharmonic approximation, does not allow one to describe well the high-temperature experimental data.

For Pt the temperature dependence of the adiabatic bulk modulus was determined in Ref. 74, but the results appeared to be internally inconsistent. The filled squares are values $K_S(T)$ from Fig. 1 in Ref. 74 (these were used by us), and empty squares—computed from the polynomial from Table 1 in Ref. 74. For gold (Ref. 72) such a contradiction did not appear.

Table I also shows the parameters of the EOSs of Ag, diamond, and MgO. The EOS of Ag is an update of our earlier version;²¹ the EOS of periclase will be discussed

TABLE I. Parameters of the proposed EOSs.

Parameters	Ag	Al	Au	Cu	Pt	Ta	W	MgO	Diamond
V_0 (cm ³)	10.272	9.999	10.215	7.113	9.091	10.851	9.545	11.248	3.417
K_0 (GPa)	99.65	72.67	166.70	133.41	276.07	191.39	306.00	160.31	443.16
K'	6.11	4.62	6.00	5.37	5.30	3.81	4.17	4.18	3.777
Θ_{B1} (K)	130.6	245.8	95.7	123.7	95.2	72.6	182.8	447.3	1202.1
d_{B1}	8.572	5.575	8.290	3.776	8.199	5.536	13.270	11.248	9.604
m_{B1}	0.121	0.987	0.681	0.115	0.329	0.117	0.513	1.429	1.163
Θ_{B2} (K)	103.6	–	106.4	175.4	148.4	101.8	172.5	384.0	1135.1
d_{B2}	5.326	–	3.239	10.372	4.005	24.513	3.305	3.593	3.380
m_{B2}	0.449	–	0.417	0.711	0.383	0.396	0.174	0.276	0.218
Θ_{E1} (K)	111.9	240.2	170.6	187.4	214.6	144.0	287.6	703.8	1687.2
m_{E1}	0.766	1.000	1.063	0.756	1.211	1.118	1.166	2.570	1.396
Θ_{E2} (K)	189.12	356.2	105.2	286.9	140.8	214.9	213.8	466.0	1033.7
m_{E2}	1.664	1.013	0.839	1.418	1.077	1.369	1.145	1.725	0.223
γ_0	2.376	2.144	2.965	1.974	2.802	1.714	1.553	1.522	0.820
γ_∞	1.481	1.017	1.142	1.554	1.538	1.241	0.694	1.111	0.615
β	2.507	3.942	3.030	4.647	5.550	6.825	3.698	4.509	10.121
a (10 ⁻⁶ K ⁻¹)	6.70	5.14	25.33	3.50	160.9	61.9	-39.3	13.56	-23.85
m	3.44	3.44	3.79	3.46	4.06	4.00	2.67	5.23	1.22
e (10 ⁻⁶ K ⁻¹)	25.9	54.1	18.92	27.698	260.0	167.0	40.4	–	–
g	0.666	1.8 ^a	0.66	0.666	2.4 ^a	1.3 ^a	0.2 ^a	–	–
H (K)	15239	8679	11.69	11687	32572	36278	14714	–	–
S	0.732	0.998	1.067	1.407	0.631	4.910	0.672	–	–

^aReference 31.

elsewhere,⁹⁶ and the EOS of diamond has been constructed in view of its frequent use for creating pressure scales. The EOS of diamond was based on shock-wave data and experimental measurements of C_p , α , K_S . The obtained value of $K' = 3.77$ (Table I) turns out to be close to the results of Kunc *et al.*^{22,23} and coincides with results of *ab initio* calculations of Oganov (unpublished).

Let us analyze in more detail Fig. 6(b), which shows the differences between the calculated and measured low-temperature heat capacity of W. These differences for all the considered substances basically do not exceed 1%, therefore the calculated standard entropy of tungsten $S_{298} = 32.65$ J mol⁻¹ K⁻¹ coincides with the reference data: $S_{298} = 32.64 \pm 0.42$ J mol⁻¹ K⁻¹ (Ref. 97) and $S_{298} = 32.66$ J mol⁻¹ K⁻¹ (Ref. 48). For other substances the entropies are (in brackets we give the measured entropies from Ref. 97) Ag 42.72 (42.55 ± 0.21), Al 28.31 (28.35 ± 0.09), Au 47.35 (47.49 ± 0.21), Cu 33.16 (33.15 ± 0.08), Pt 41.45 (41.63 ± 0.21), Ta 41.50 (41.51 ± 0.17), MgO 26.96 (26.94 ± 0.17), and for diamond 2.366 (2.38 ± 0.01) J mol⁻¹ K⁻¹. Therefore the constructed EOSs can also be used for a compact representation of thermodynamic functions of substances without phase transitions from 10–15 K up to the melting temperature at room pressure.

Figure 8 shows the deviations of the calculated pressure on room-temperature isotherms from selected experimental (without recalibration) and theoretical data. The deviations of

data of Dewaele *et al.*^{24,26} for Al, Au, Cu, Pt, Ta, and W recalibrated using the scale (16) are very small, like those shown in Fig. 4. In the work of Chijioke *et al.*,⁴³ shock-wave data were used for calculation of room-temperature isotherms of Al, Cu, Ta, and W. They used ultrasonic measurements of bulk moduli at low pressure and considered the effect of stress in the shock-wave data, however, their room-temperature isotherms do not always coincide with ours. At the same x , the pressure on room-temperature isotherms⁴³ is higher than found here for Al and Pt, lower for Au, Cu, and W [Fig. 6(e)] and almost coincides for Ta. A similar situation occurs with the room-temperature isotherms reduced from shock-wave data in Refs. 29 and 56, except Al, for which data of Ref. 56 are in excellent agreement with our results.

The room-temperature isotherms reduced from the shock-wave data of Carter *et al.*¹⁰ agree with ours up to 100 GPa for Cu and Ag, but above 100 GPa the pressure from Ref. 10 is higher. Figure 8 also shows unpublished data of Dewaele *et al.*⁸⁶ for Ag, measured at the same conditions as in Ref. 24. Deviations of these data are shown in two variants: first, calibrating the pressure with the scale,²⁴ second, using our scale (16). These measurements confirm, once again, the most recent calibrations of the ruby pressure scale.

For Ta the room-temperature isotherms^{29,43} reduced from shock-wave data agree well with our isotherms. In the measurements of Cynn and Yoo,⁸⁴ carried out in the argon medium, the pressure was determined using the gold pressure scale with parameters $K_0 = 166.6$ GPa and $K' = 5.5$. In Fig. 8 these data are shown after recalculation using the EOS of Au

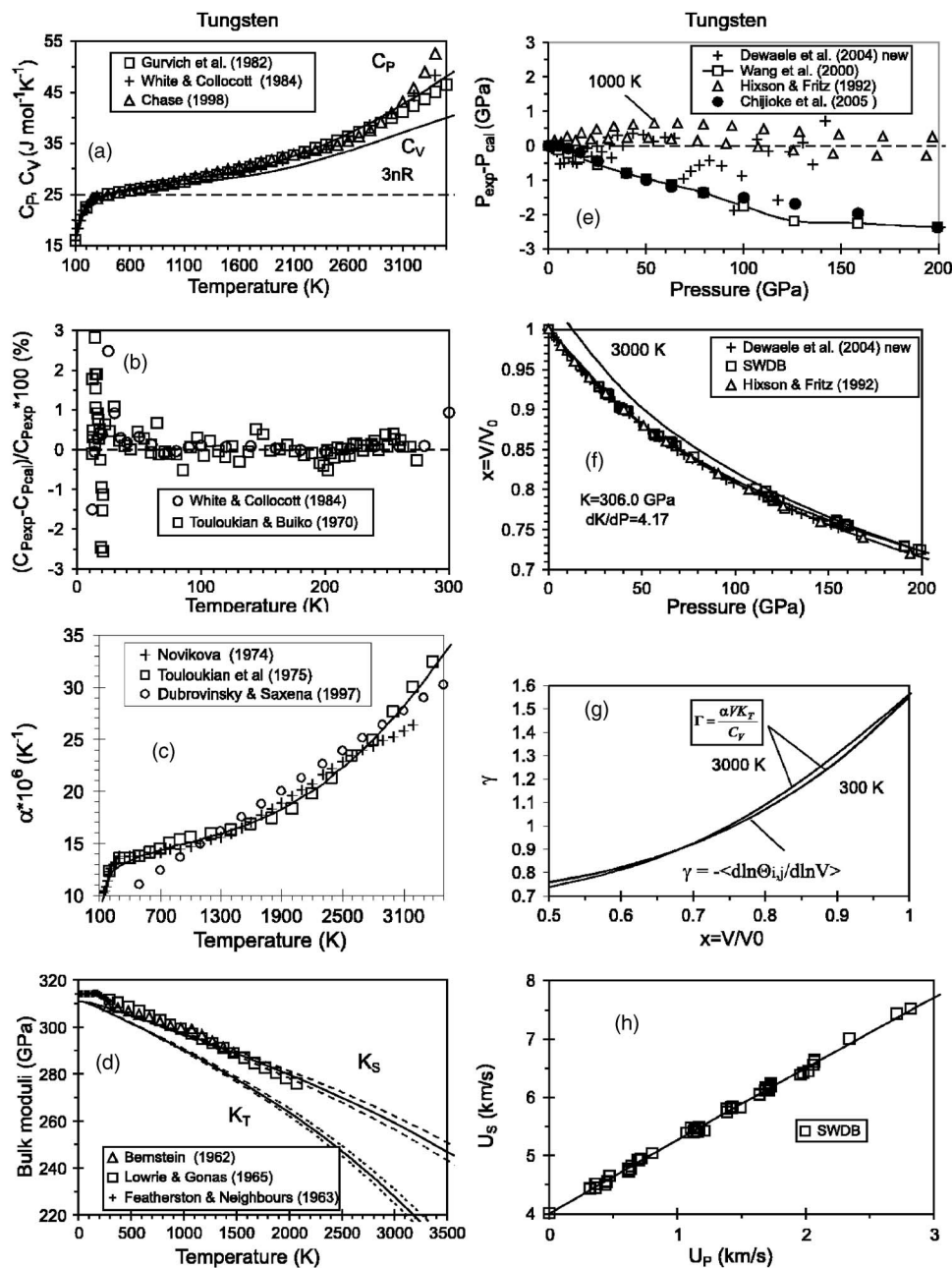


FIG. 6. Comparison of thermodynamic functions of tungsten calculated from our EOS (parameters from Table I) with experimental and theoretical data. (a) C_p and C_v , experimental data from Refs. 46–48. (b) Relative deviations of the calculated C_p from experimental measurements (Refs. 47 and 49). (c) Thermal expansion coefficient in comparison with Refs. 50–52. (d) Bulk moduli in comparison with Refs. 53–55; dotted lines correspond to the variation of K' in the range ± 0.2 . (e) Deviations of the calculated pressure from experimental and theoretical data (Refs. 24, 56, 28, and 43). (f) Calculated 300 and 3000 K isotherms and shock adiabats in comparison with experiments (Refs. 24, 30, and 28). (g) Grüneisen parameters. (h) Calculated shock-wave velocity versus particle velocity in comparison with the Shock Wave Database (Ref. 30).

(Table I); one can see that the recalculated isotherm⁸⁴ agrees with ours. In the measurements of Hanfland *et al.*,⁸³ carried out in the neon and Na pressure medium, pressure was calculated using the ruby scale of Mao *et al.*⁶ Figure 8 shows the deviation of the isotherms⁸³ calculated using two set of parameters: $K_0=207.6$ GPa, $K'=2.85$ and $K_0=199$ GPa, $K'=3.95$.

We have slightly modified our previous version^{45,98} of the equations of state of gold and MgO, taking into account the measurements of Refs. 89 and 90 in He pressure-transmitting medium and measurements of Ref. 43 in hydrogen pressure-transmitting medium. Pressures in Fig. 8 are calculated for these data using the ruby scale (16). It turned out that cell parameters calculated from (111) and (200) x-ray reflections⁸⁹ are significantly different, which contributes to the uncertainty in pressure calibration. The adopted value

$K'=6.0$ for gold (Table I) is consistent with measurements from Refs. 24, 43, and 90 and with pressure calculated from (111) reflections.⁸⁹ For Pt we see a satisfactory agreement between the isotherms in Fig. 8, except the isotherm of Ref. 99, where the recommended $K'=4.8 \pm 0.3$ is much lower than our value $K'=5.3$.

The deviations of the room-temperature isotherms of MgO from the measurements of Speziale *et al.*⁹³ are shown in Fig. 8 in two variants: the original data,⁹³ where the pressure was determined using the Mao *et al.*⁶ scale, and recalibrated using Eq. (16). The ideal consistency of the recalibrated isotherm is achieved with $K'=4.4$, but this leads to inconsistencies with other measurements,^{19,100} which will be considered elsewhere.⁹⁶ Figure 8 also shows the differences between the measurements of Occelli *et al.*²⁵ for diamond recalibrated using Eq. (16), and the room-temperature iso-

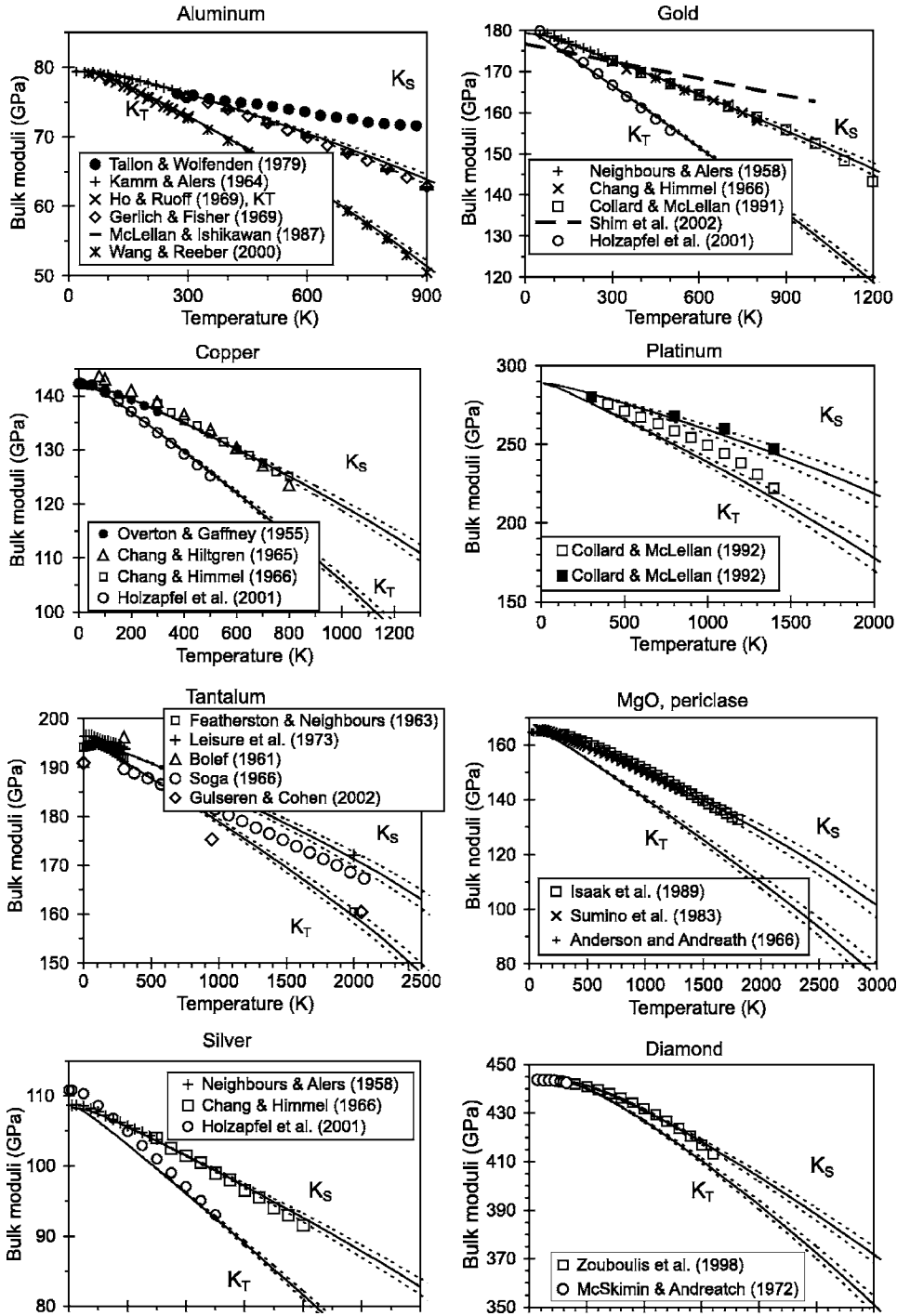


FIG. 7. Comparison of the calculated bulk moduli of Al, Cu, Ta, Ag, Au, Pt, diamond, and MgO with ultrasonic measurements [for tungsten see Fig. 6(d)]. Dotted lines correspond to the variation of K' in the range ± 0.2 , except platinum for which the range ± 0.5 is shown; the top dotted line corresponds to the lower value of K' . Experimental data are from Refs. 57–62 for Al, Refs. 63–66 for Cu, Refs. 55 and 67–70 for Ta, Refs. 71, 65, and 66 for Ag, Refs. 71, 65, 72, 73, and 66 for Au, Ref. 74 for Pt, Refs. 75–77 for MgO, and Refs. 78 and 15 for diamond.

therm of diamond with parameters $K_0=443.2$ GPa and $K'=3.77$ (Table I).

Summing up, for a number of reference materials we have developed a unified thermodynamic model capable of describing a very diverse set of experimental data (thermochemistry, P - V - T EOSs, ultrasonic measurements) within the experimental error bars. The room-temperature isotherms of reference metals allowed us to recalibrate the ruby pressure scale. The proposed scale in the form (16) agrees very well with the recalibrated measurements of Dewaele *et al.*,²⁴ and is consistent with independent quasi-hydrostatic measurements, but only when these measurements are recalibrated.

IV. DISCUSSION AND SUMMARY

Let us compare recent ruby pressure scales extrapolated to 300 GPa and discuss the importance of the chosen functional form of $P(\lambda)$ (Fig. 9). At given λ we have calculated pressure (and its deviations from our scale). The scatter of the calculated pressures exceeds ± 30 GPa at a pressure of 300 GPa, but is much smaller for ruby scales published after 2003.

At the pressure of 150 GPa all recent scales described by various functional dependences are consistent within ± 3 –4 GPa, but at higher pressures they begin to diverge. In

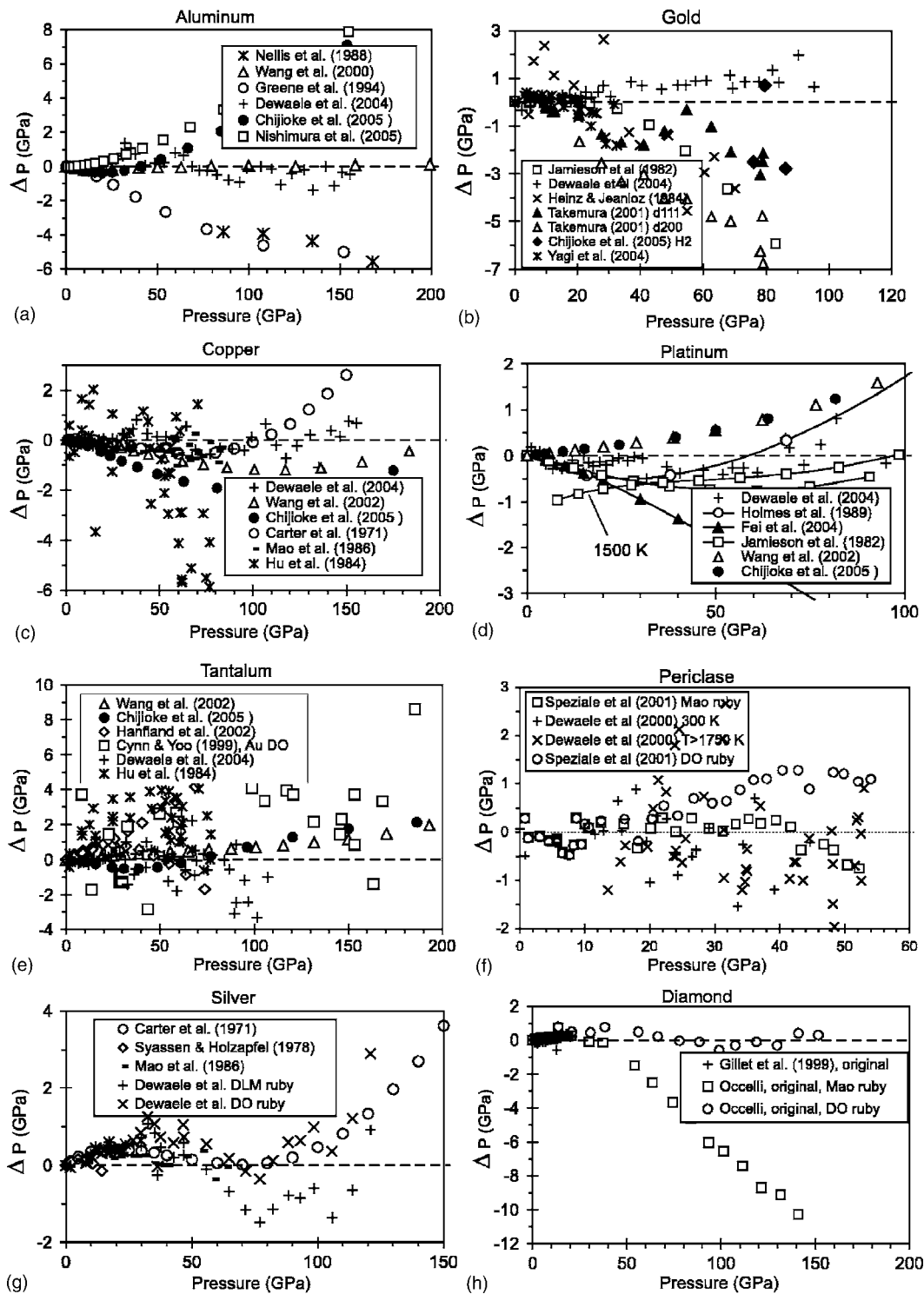


FIG. 8. Differences between our calculated room-temperature isotherms (Table I) and previous determinations: $\Delta P = P_{old} - P_{new}$. “DO ruby” means calibration done with the present ruby scale. Experimental and theoretical data are from Refs. 79, 56, 80, 24, 43, and 81 for Al, Refs. 56, 24, 29, 43, 10, 6, and 82 for Cu, Refs. 43, 83, 84, 24, 26, and 82 for Ta, Refs. 10, 85, 6, and 86 for Ag (see text), Refs. 87, 24, 88, 43, 89, and 90 for Au, Refs. 24, 91, 92, 87, 29, and 43 for Pt, Refs. 93 and 94 for MgO, and Refs. 95 and 25 for diamond.

our view, this is largely related to the different forms of $P(\lambda)$, which is easily seen in the example of our scale in the form Eq. (1) with parameters $A=1885$ GPa and $B=11$ (Fig. 3) which as we mentioned, is good up to 85 GPa, and above 85 GPa has parameters $A=1975$ GPa and $B=8.59$. However,

instead of these two scales it is sufficient to use a single scale described by Eq. (16) and recommended here.

The scale of Chijioke *et al.*⁴³ in the form Eq. (1) at pressures above 120 GPa considerably deviates from our scale (16). However, they also represented their scale by Eq. (4)

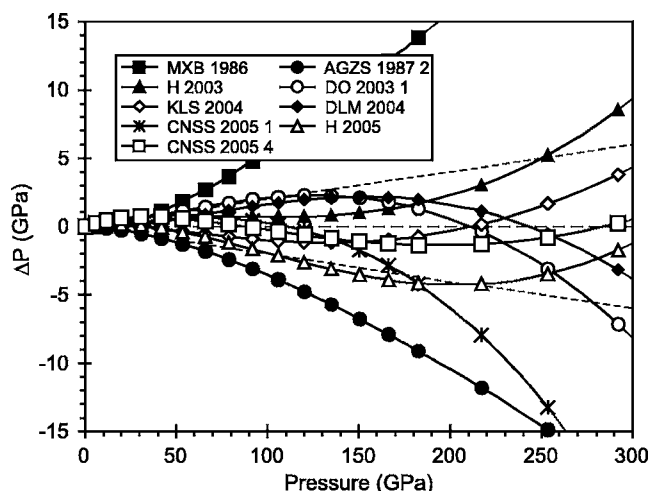


FIG. 9. Difference between published ruby scales extrapolated to pressure 300 GPa at given value λ : $\Delta P = P_{\text{Eq. (16)}} - P_{\text{other}}$. MBX 1986—Mao *et al.* (Ref. 6) AGZS 1987 2—Aleksandrov *et al.* (Ref. 12) calibration using Eq. (2) with parameters $A = 1892 \pm 13$ GPa and $m = 6.4$; H 2003—Holzapfel (Ref. 20), DO 2003 1—Dorogokupets and Oganov (Ref. 21) calibration using Eq. (1) with parameters $A = 1871$ GPa and $B = 10.06$; KLS 2004—Kunc *et al.* (Refs. 22, 23, and 41) calibration in the form $P = 1860 \times (\Delta\lambda/\lambda)[1 + 7.75(\Delta\lambda/\lambda)]$; DLM 2004—Dewaele *et al.* (Ref. 24) calibration using Eq. (1) with parameters $A = 1904$ GPa and $B = 9.5$; CNSS 2005 1—Chijioko *et al.* (Ref. 43) calibration using Eq. (1) with parameters $A = 1873 \pm 6.7$ GPa and $B = 10.82 \pm 0.14$; H 2005—Holzapfel (Ref. 44) CNSS 2005 4—Chijioko *et al.* (Ref. 43) calibration in the form $P = 1794 \times (\Delta\lambda/\lambda)[1 + 8.68(\Delta\lambda/\lambda)]$. Dashed lines correspond to $\pm 2\%$ deviations.

with parameters $A = 1794 \pm 8.4$ GPa and $\mu = 8.68 \pm 0.15$; this function is consistent with our scale (16) also above 120 GPa and does not contradict recommendations of other authors.

The ruby pressure scale in the form (4) is discussed in Refs. 20, 22, 23, and 41. These authors remark that the two-parametrical scale (4) with $A = 1820$ GPa and $\mu = 7.9$ practically coincides with the three-parametrical scale of Holzapfel²⁰ up to a pressure of 200 GPa. At the same time Kunc *et al.*^{22,23,41} recommended a ruby pressure scale in the form (4) with parameters $A = 1860$ GPa and $\mu = 7.75$, which agrees with our scale to within 1% (Fig. 9).

Holzapfel⁴⁴ has re-analyzed the data of Dewaele *et al.*²⁴ and Occelli *et al.*²⁵ and has obtained a ruby pressure scale with parameters $A = 1845$ GPa, $B = 14.7$, $C = 7.5$ for Eq. (3), which rather considerably differs from his previous ruby pressure scale,²⁰ but deviations from our scale only slightly exceed 2% in the range 100–220 GPa.

From the comparison of the proposed ruby pressure scale (16) and the scale of Chijioko *et al.*⁴³ in the form (4) it is possible to draw conclusions about the most appropriate functional form for $P(\lambda)$. If one considers these scales as closest to the truth, then the scale (16) in the form (2) has doubtless advantage of having the parameter $A = 1884$ GPa close to the direct measurement $A = 1875 \pm 30$ GPa in Ref. 39. The scale of Chijioko *et al.*⁴³ in the form (4) has a considerably smaller value of the parameter $A = 1794 \pm 8.4$ GPa, which is very different from direct measurements at low pressure.³⁹

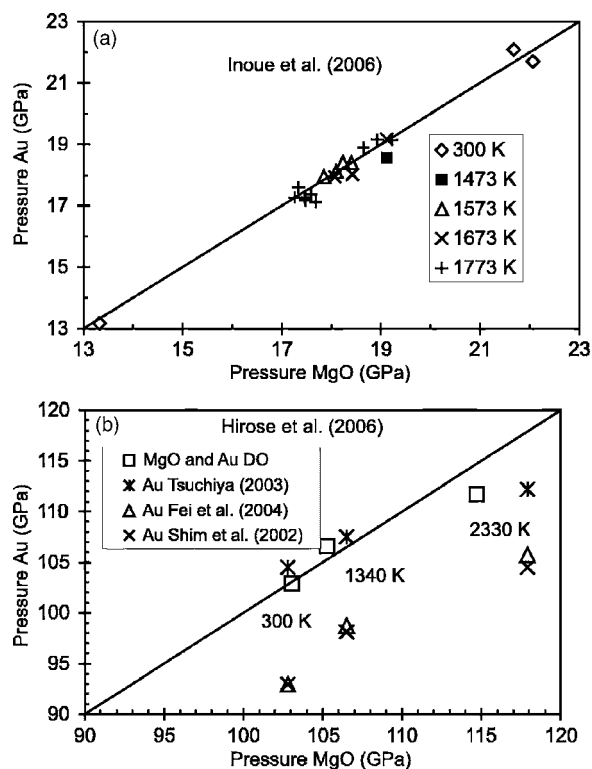


FIG. 10. Comparison of MgO and Au pressure scale (Tables IV and IX) with other pressure scales. (a) compares our Au and MgO pressure scales using measurements from Ref. 105. (b) is based on measurements from Ref. 106 (done simultaneously for MgO and Au) and calibrated using our Au and MgO EOSs (DO) or using the Au pressure scales from Ref. 73 (Shim *et al.* Au EOS), Ref. 107 (Tsuchiya Au EOS), Ref. 92 (Fei *et al.* Au EOS), and MgO pressure scale from Ref. 93 (Speziale *et al.* MgO EOS).

A comparison of the room-temperature isotherms of Au and Pt, Au and Ag has been done by us earlier⁴⁵ on the basis of independent determinations of Akahama *et al.*,¹⁰¹ and has shown quite a satisfactory agreement despite the fact that measurements¹⁰¹ have been carried out in nonhydrostatic conditions. The self-consistency of our EOSs can be checked not only on room-temperature isotherms, but also at higher temperatures and pressures, using simultaneous *PVT* measurements of the unit cell parameters of MgO, Pt, and Au by Matsui and Nishiyama,¹⁰² Nishiyama *et al.*,¹⁰³ and Fei *et al.*^{92,104} Using the measured cell parameters of MgO, Pt, and Au we have calculated pressures for these materials at different temperatures. One can see (Fig. 9 in Ref. 45) excellent agreement with the data of Fei *et al.*,^{92,104} whereas some systematic difference is present for the measurements from Refs. 102 and 103. Very recent studies of Inoue *et al.*¹⁰⁵ and Hirose *et al.*¹⁰⁶ give us a possibility to compare the EOSs of Au and MgO at very high P - T parameters. Figure 10(a) compares the pressure scales of MgO and Au, calculated from the measurements of Inoue *et al.*¹⁰⁵ and checked against our Au and MgO EOSs at temperatures from 300 to 1773 K and pressures from 13 up to 22 GPa. Figure 10(b) compares the pressure scales of MgO and Au at pressures above 100 GPa based on the measurements of Hirose *et al.*,¹⁰⁶ where EOSs

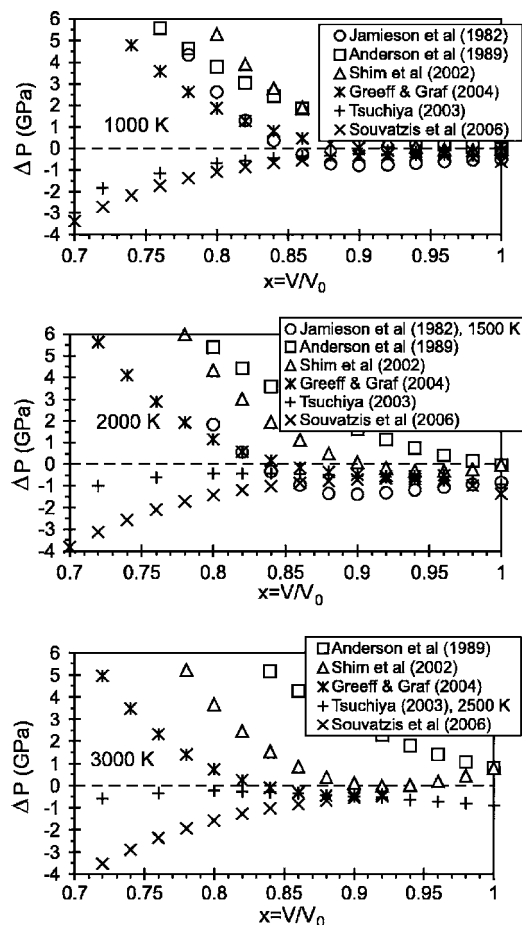


FIG. 11. The difference $\Delta P = P_{\text{DO}} - P_{\text{other}}$ between calculated pressure (Table IV) on 1000, 2000, and 3000 K isotherms of Au and pressures from Jamieson *et al.* (Ref. 87), Anderson *et al.* (Ref. 108), Shim *et al.* (Ref. 73), Tsuchiya (Ref. 107), Greeff and Graf (Ref. 110), and Souvatzis *et al.* (Ref. 109). EOSs of gold, plotted against normalized unit-cell volume (see pressure at given $x = V/V_0$ in Table IV).

of MgO (Ref. 93) and Au (Ref. 107) have been compared. While Au EOS (Ref. 107) gives pressures up to 5 GPa lower than MgO EOS (Ref. 93) at 2330 K, our EOSs of MgO and Au differ by less than 3 GPa. Comparing MgO EOS (Ref. 93) and Au EOSs from Refs. 73 and 92 one can see that Au EOS from Refs. 73 and 92 underestimate pressure at 2330 K by ~ 10 GPa in comparison with MgO EOS.⁹³

Finally, let us comment on the EOS of Au, which has been recommended as a primary pressure standard at elevated temperatures,⁸⁷ but for which very different EOSs have been suggested in subsequent works (Refs. 108 and 73). The differences between our data and previously published room-temperature isotherms of Au in coordinates $\Delta P - P$ is shown in Fig. 8, and Fig. 11 shows the differences on 1000, 2000, and 3000 K isotherms in coordinates $\Delta P - x$. While the differences at room temperature are entirely due to the difference in K_0 and K' , at elevated temperatures errors in the thermal pressure must also be considered. In Ref. 108, thermal pressure was evaluated using empirical relations leading to large differences from our results. We find good agreement with the results of first-principles calculations of Refs. 107

and 109 especially at high temperatures, but there are differences from calculations of Ref. 110, where for the room-temperature isotherm $K' = 5.5$ was adopted. We suggest that the EOS of gold reported in Table IV gives a reliable pressure standard.

Another popular pressure standard, platinum, is less preferable because at high pressures and temperatures it was found to react with diamond forming PtC (Ref. 111) and because of the uncertainty in the temperature dependence of the adiabatic bulk modulus (see Ref. 74 and discussion in the text).

Tables II–X with the calculated isotherms of Ag, Al, Cu, Pt, Ta, W, MgO, and diamond extending to ~ 200 GPa and 3000 K are given in the Appendix.¹¹² We recommend these tables for pressure calibration in this $P - T$ range.

V. CONCLUDING REMARKS

We have obtained internally consistent semiempirical EOSs of Al, Au, Cu, Pt, Ta, W, and MgO in a wide pressure-temperature range on the basis of a simultaneous analysis of thermochemical, x-ray, ultrasonic, and shock-wave data. Our EOSs are consistent with all recent experimental data. The EOSs of Al, Au, Cu, Pt, Ta and W, combined with the precise measurements of Dewaele *et al.*,^{24,26} allowed us to obtain a new calibration of the ruby pressure scale. The cross check with the independent data of Matsui and Nishiyama,¹⁰² Nishiyama *et al.*,¹⁰³ Fei *et al.*,^{92,104} Inoue *et al.*,¹⁰⁵ and Hirose *et al.*¹⁰⁶ confirms the obtained EOSs of Al, Au, Cu, Pt, Ta, W, and MgO.

The revised ruby pressure scale has a simple functional form capable of representing the $P(\lambda)$ dependence in the whole pressure range 0–300 GPa by a single equation. The obtained ruby pressure scale agrees to within 2% with other recent ruby pressure scales (Refs. 20–24, 41, 43, and 44), but has a number of advantages. First, it is consistent with room-temperature isotherms of Al, Au, Cu, Pt, Ta, and W obtained here on the basis of our unified thermodynamic formalism. Second, it does not contradict recent EOSs of diamond.^{22,23,41,113} Third, and most important, the obtained $P - V - T$ EOSs enable consistent pressure calibration using either the ruby scale or EOSs of any of the reference substances studied here (Ag, Al, Au, Cu, Pt, Ta, W, diamond, MgO). This solves problems of inconsistency between different pressure scales and enables accurate pressure calibration at elevated temperatures, where the ruby scale cannot be used.

ACKNOWLEDGMENTS

P.I.D. is grateful to Academician F.A. Letnikov (Irkutsk, Russia) for support of his research and P. Richet (IPGP, Paris, France) for support at IPGP. Special thanks to A. Dewaele and P. Loubeyre (CEA/DAM, Bruyeres-le-Chatel, France) for their new and unpublished data on silver. We thank K. Takemura for unpublished data on gold. This work was supported by the Russian Foundation for Basic Research, Grant No. 05-05-64491.

APPENDIX

TABLE II. Isochors for Ag. Pressure (in GPa) as a function of compression ($x=V/V_0$) and temperature (K).

$x=V/V_0$	298.15	1000	2000	2500
1	0.000	4.013	9.791	12.786
0.95	5.972	9.999	15.797	18.771
0.9	14.419	18.475	24.325	27.297
0.85	26.319	30.421	36.353	39.350
0.8	43.076	47.244	53.294	56.340
0.75	66.745	70.998	77.206	80.328
0.7	100.371	104.735	111.146	114.371
0.65	148.568	153.067	159.735	163.093
0.6	218.470	223.132	230.123	233.648

TABLE III. Isochors for Al.

$x=V/V_0$	298.15	1000	2000	2500
1	0.000	3.764	10.168	13.913
0.95	4.193	7.747	13.739	17.301
0.9	9.736	13.118	18.744	22.121
0.85	17.061	20.310	25.629	28.817
0.8	26.767	29.917	35.000	38.004
0.75	39.684	42.771	47.699	50.537
0.7	56.986	60.046	64.905	67.613
0.65	80.366	83.432	88.314	90.947
0.6	112.309	115.417	120.410	123.039
0.55	156.562	159.749	164.941	167.640
0.5	218.931	222.232	227.716	230.556

TABLE IV. Isochors for Au.

$x=V/V_0$	298.15	1000	2000	2500
1	0.00	4.96	12.11	15.96
0.95	9.96	14.72	21.55	25.20
0.9	23.98	28.57	35.12	38.58
0.85	43.65	48.08	54.42	57.71
0.8	71.21	75.53	81.71	84.87
0.75	109.98	114.21	120.29	123.36
0.7	164.83	169.00	175.03	178.06
0.65	243.11	247.25	253.31	256.35

TABLE V. Isochors for Cu.

$x=V/V_0$	298.15	1000	2000	2500
1	0.000	4.789	12.152	16.534
0.95	7.845	12.644	19.909	24.143
0.9	18.575	23.424	30.683	34.791
0.85	33.222	38.161	45.510	49.536
0.8	53.237	58.308	65.844	69.848
0.75	80.689	85.932	93.753	97.810
0.7	118.576	124.032	132.235	136.428
0.65	171.322	177.032	185.717	190.127
0.6	245.599	251.600	260.876	265.581

TABLE VI. Isochors for Pt.

$x=V/V_0$	298.15	1000	2000	3000
1	0.000	5.309	12.864	20.349
0.95	16.207	21.219	28.485	35.822
0.9	38.307	43.111	50.199	57.476
0.85	68.389	73.069	80.079	87.376
0.8	109.388	114.016	121.043	128.434
0.75	165.473	170.119	177.253	184.808
0.7	242.676	247.403	254.730	262.523

TABLE VII. Isochors for Ta.

$x=V/V_0$	298.15	1000	2000	3000
1	0.000	2.709	6.538	10.351
0.95	10.818	13.465	17.274	21.111
0.9	24.582	27.219	31.074	35.009
0.85	42.131	44.803	48.762	52.855
0.8	64.588	67.334	71.451	75.749
0.75	93.474	96.332	100.654	105.203
0.7	130.887	133.891	138.468	143.309
0.65	179.768	182.953	187.836	193.013
0.6	244.325	247.727	252.971	258.537

TABLE VIII. Isochors for W.

$x=V/V_0$	298.15	1000	2000	3000
1	0.000	2.934	7.461	12.670
0.95	17.456	20.238	24.520	29.361
0.9	40.047	42.703	46.783	51.310
0.85	69.323	71.877	75.797	80.072
0.8	107.377	109.855	113.658	117.743
0.75	157.082	159.512	163.239	167.200
0.7	222.444	224.854	228.550	232.448

TABLE IX. Isochors for MgO.

$x=V/V_0$	298.15	1000	2000	3000
1	0.000	4.174	10.354	16.286
0.95	9.147	13.263	19.478	25.516
0.9	20.988	25.076	31.374	37.560
0.85	36.338	40.425	46.857	53.236
0.8	56.295	60.409	67.029	73.651
0.75	82.371	86.534	93.401	100.325
0.7	116.670	120.904	128.081	135.372
0.65	162.179	166.501	174.059	181.794
0.6	223.226	227.647	235.665	243.935

TABLE X. Isochors for diamond.

$x=V/V_0$	298.15	1000	2000	3000
1	0.000	2.706	8.466	14.788
0.95	25.028	27.518	32.942	38.930
0.9	56.828	59.201	64.491	70.359
0.85	97.318	99.641	104.940	110.843
0.8	149.061	151.377	156.790	162.847
0.75	215.532	217.870	223.477	229.779
0.7	301.514	303.890	309.757	316.383

*Electronic mail: dor@crust.irk.ru

†Electronic mail: a.oganov@mat.ethz.ch

- ¹C. E. Weir, E. R. Lippincott, A. Van Valkenburg, and E. N. Bunting, *J. Res. Natl. Bur. Stand., Sect. A* **63A**, 55 (1959); J. C. Jamieson, A. W. Lawson, and N. D. Nachtrieb, *Rev. Sci. Instrum.* **30**, 1016 (1959).
- ²R. A. Forman, G. J. Piermarini, J. D. Barnett, and S. Block, *Science* **176**, 284 (1972).
- ³G. J. Piermarini, S. Block, J. D. Barnett, and R. A. Forman, *J. Appl. Phys.* **46**, 2774 (1975).
- ⁴G. J. Piermarini and S. Block, *Rev. Sci. Instrum.* **46**, 973 (1975).
- ⁵H. K. Mao, P. M. Bell, J. W. Shaner, and D. J. Steinberg, *J. Appl. Phys.* **49**, 3276 (1978).
- ⁶H. K. Mao, J. P. Xu, and P. Bell, *J. Geophys. Res.* **91**, 4673 (1986).
- ⁷A. Jayaraman, *Rev. Mod. Phys.* **55**, 65 (1983).
- ⁸A. Jayaraman, *Rev. Sci. Instrum.* **57**, 1013 (1986).
- ⁹G. J. Piermarini, *J. Res. Natl. Inst. Stand. Technol.* **106**, 889 (2001).
- ¹⁰W. J. Carter, S. P. Marsh, J. N. Fritz, and R. G. McQueen, in *Accurate Characterization of the High Pressure Environment*, edited by E. C. Lloyd (National Bureau of Standards, Washington, DC, 1971), NBS Spec. Publ., Vol. 326, p. 147.
- ¹¹D. L. Decker, *J. Appl. Phys.* **42**, 3239 (1971).
- ¹²I. V. Aleksandrov, A. F. Goncharov, A. N. Zisman, and S. M. Stishov, *Zh. Eksp. Teor. Fiz.* **93**, 680 (1987) [*Sov. Phys. JETP* **66**, 384 (1987)].
- ¹³O. H. Nielsen, *Phys. Rev. B* **34**, 5808 (1986).
- ¹⁴M. Hanfland, K. Syassen, S. Fahy, S. G. Louie, and M. L. Cohen, *Phys. Rev. B* **31**, 6896 (1985).
- ¹⁵H. J. McSkimin and P. Andreatch, *J. Appl. Phys.* **43**, 2944 (1972).
- ¹⁶R. J. Hemley, C. S. Zha, A. P. Jephcoat, H. K. Mao, L. W. Finger, and D. E. Cox, *Phys. Rev. B* **39**, 11820 (1989).
- ¹⁷R. G. McQueen, S. P. Marsh, J. W. Taylor, J. N. Fritz, and W. J. Carter, in *High-Velocity Impact Phenomena*, edited by R. Kin-slow (Academic, New York, 1970), p. 293.
- ¹⁸P. M. Bell and H. K. Mao, *Carnegie Inst. Washington Publ.* **80**, 404 (1981).
- ¹⁹C. S. Zha, H. K. Mao, and R. J. Hemley, *Proc. Natl. Acad. Sci. U.S.A.* **97**, 13494 (2000).
- ²⁰W. B. Holzapfel, *J. Appl. Phys.* **93**, 1813 (2003).
- ²¹P. I. Dorogokupets and A. R. Oganov, *Dokl. Earth Sci.* **391A**, 854 (2003).
- ²²K. Kunc, I. Loa, and K. Syassen, *Phys. Rev. B* **68**, 094107 (2003).
- ²³K. Kunc, I. Loa, and K. Syassen, *High Press. Res.* **24**, 101 (2004).
- ²⁴A. Dewaele, P. Loubeyre, and M. Mezouar, *Phys. Rev. B* **70**, 094112 (2004).
- ²⁵F. Occelli, P. Loubeyre, and R. Letoullec, *Nat. Mater.* **2**, 151 (2003).
- ²⁶A. Dewaele, P. Loubeyre, and M. Mezouar, *Phys. Rev. B* **69**, 092106 (2004).
- ²⁷W. J. Nellis, J. A. Moriarty, A. C. Mitchell, M. Ross, R. G. Dandrea, N. W. Ashcroft, N. C. Holmes, and G. R. Gather, *Phys. Rev. Lett.* **60**, 1414 (1988).
- ²⁸R. S. Hixson and J. N. Fritz, *J. Appl. Phys.* **71**, 1721 (1992).
- ²⁹Y. Wang, R. Ahuja, and B. Johansson, *J. Appl. Phys.* **92**, 6616 (2002).
- ³⁰K. V. Khishchenko, P. R. Levashov and I. V. Lomonosov, *Shock Wave Database*. Available from <http://teos.ficp.ac.ru/rusbank>(2001).
- ³¹V. N. Zharkov and V. A. Kalinin, *Equations of State of Solids at High Pressures and Temperatures* (Consultants Bureau, New York, 1971).
- ³²P. Vinet, J. Ferrante, J. Rose, and J. Smith, *J. Geophys. Res.* **92**, 9319 (1987).
- ³³A. M. Kut'in and D. V. Pyadushkin, *Russ. J. Phys. Chem.* **72**, 1567 (1998).
- ³⁴A. M. Kut'in, D. V. Pyadushkin, and E. A. Bykova, *Russ. J. Phys. Chem.* **72**, 1573 (1998).
- ³⁵L. V. Al'tshuler, S. E. Brusnikin, and E. A. Kuz'menkov, *J. Appl. Mech. Tech. Phys.* **28**, 129 (1987).
- ³⁶A. R. Oganov and P. I. Dorogokupets, *J. Phys.: Condens. Matter* **16**, 1351 (2004).
- ³⁷M. I. Katsnelson, A. F. Maksyutov, and A. V. Trefilov, *Phys. Met. Metallogr.* **95**, 304 (2003).
- ³⁸K. Wang and R. R. Reeber, *Mater. Sci. Eng., R.* **R23**, 101 (1998).
- ³⁹O. Grasset, *High Press. Res.* **21**, 139 (2001).
- ⁴⁰K. Nakano, Y. Akahama, Y. Ohishi, and H. Kawamura, *Jpn. J. Appl. Phys.* **39**, 1249 (2000).
- ⁴¹K. Syassen, unpublished notes (2005).
- ⁴²N. Funamori and R. Jeanloz, *Science* **278**, 1109 (1997); T. Mashimo, K. Tsumoto, K. Nakamura, Y. Noguchi, K. Fukuoka, and Y. Syono, *Geophys. Res. Lett.* **27**, 2021 (2000); J. F. Lin, O. Degtyareva, C. T. Prewitt, P. Dera, N. Sata, E. Gregoryanz, H. K. Mao, and R. J. Hemley, *Nat. Mater.* **3**, 389 (2004); A. R. Oganov and S. Ono, *Proc. Natl. Acad. Sci. U.S.A.* **102**, 10828 (2005); R. Caracas and R. E. Cohen, *Geophys. Res. Lett.* **32**, L06303 (2005); J. Tsuchiya, T. Tsuchiya, and R. M. Wentzcovitch, *Phys. Rev. B* **72**, 020103 (2005).
- ⁴³A. D. Chijioke, W. J. Nellis, A. Soldatov, and I. F. Silvera, *J. Appl. Phys.* **98**, 073526 (2005); **98**, 114905 (2005).
- ⁴⁴W. B. Holzapfel, *High Press. Res.* **25**, 187 (2005).
- ⁴⁵P. I. Dorogokupets and A. R. Oganov, in *Proceedings Joint 20th AIRAPT & 43th EHPRG International Conference on High Pressure Science and Technology*, 27 June–1 July 2005, Karlsruhe Germany (Forschungszentrum Karlsruhe, Karlsruhe, 2005).
- ⁴⁶L. V. Gurvich, I. V. Veiz, V. A. Medvedev *et al.*, *Thermodynamic Properties of Individual Substances* (Nauka, Moscow, 1981), Vol. 4, Book 2.
- ⁴⁷K. White and S. Collocott, *J. Phys. Chem. Ref. Data* **13**, 1251 (1984).
- ⁴⁸M. W. Chase, Jr., *NIST-JANAF Thermochemical Tables*. 4th Ed., *J. Phys. Chem. Ref. Data Monogr. No. 9* (1998).
- ⁴⁹Y. S. Touloukian and E. H. Buiko, in *Thermophysical Properties of Matter* (Plenum Press, New York, 1970), Vol. 4.
- ⁵⁰S. I. Novikova, *Thermal Expansion of Solids* (Nauka, Moscow, 1974), in Russian.
- ⁵¹Y. S. Touloukian, R. K. Kirby, R. E. Taylor, and P. D. Desai, in *Thermophysical Properties of Matter* (Plenum, New York, 1975), Vol. 12.
- ⁵²L. S. Dubrovinsky and S. K. Saxena, *Phys. Chem. Miner.* **24**, 547 (1997).
- ⁵³B. T. Bernstein, *J. Appl. Phys.* **33**, 2140 (1962).
- ⁵⁴R. Lowrie and A. M. Gonas, *J. Appl. Phys.* **36**, 2189 (1965).
- ⁵⁵F. H. Featherston and J. R. Neighbours, *Phys. Rev.* **130**, 1324 (1963).
- ⁵⁶Y. Wang, D. Chen, and X. Zhang, *Phys. Rev. Lett.* **84**, 3220

- (2000).
- ⁵⁷J. L. Tallon and A. Wolfenden, *J. Phys. Chem. Solids* **40**, 831 (1979).
- ⁵⁸G. N. Kamm and G. A. Alers, *J. Appl. Phys.* **35**, 327 (1964).
- ⁵⁹P. S. Ho and A. L. Ruoff, *J. Appl. Phys.* **40**, 3151 (1969).
- ⁶⁰D. Gerlich and E. S. Fisher, *J. Phys. Chem. Solids* **30**, 1197 (1969).
- ⁶¹R. B. McLellan and T. Ishikawan, *J. Phys. Chem. Solids* **48**, 603 (1987).
- ⁶²K. Wang and R. R. Reeber, *Philos. Mag. A* **80**, 1629 (2000).
- ⁶³W. C. Overton and J. Gaffney, *Phys. Rev.* **98**, 969 (1955).
- ⁶⁴Y. A. Chang and R. Hultgren, *J. Phys. Chem.* **69**, 4162 (1965).
- ⁶⁵Y. A. Chang and L. Himmel, *J. Appl. Phys.* **37**, 3567 (1966).
- ⁶⁶W. Holzapfel, M. Hartwig, and W. Sievers, *J. Phys. Chem. Ref. Data* **30**, 515 (2001).
- ⁶⁷R. G. Leisure, D. K. Hsu, and B. A. Seiber, *J. Appl. Phys.* **44**, 3394 (1973).
- ⁶⁸D. I. Bolef, *J. Appl. Phys.* **32**, 100 (1961).
- ⁶⁹N. Soga, *J. Appl. Phys.* **37**, 3416 (1966).
- ⁷⁰O. Gulseren and R. E. Cohen, *Phys. Rev. B* **65**, 064103 (2002).
- ⁷¹J. R. Neighbours and G. A. Alers, *Phys. Rev.* **111**, 707 (1958).
- ⁷²S. M. Collard and R. B. McLellan, *Acta Metall. Mater.* **39**, 3143 (1991).
- ⁷³S. H. Shim, T. S. Duffy, and K. Takemura, *Earth Planet. Sci. Lett.* **203**, 729 (2002).
- ⁷⁴S. M. Collard and R. B. McLellan, *Acta Metall. Mater.* **40**, 699 (1992).
- ⁷⁵D. G. Isaak, O. L. Anderson, and T. Goto, *Phys. Chem. Miner.* **16**, 704 (1989).
- ⁷⁶Y. Sumino, O. L. Anderson, and I. Suzuki, *Phys. Chem. Miner.* **9**, 38 (1983).
- ⁷⁷O. L. Anderson and P. Andreatch, *J. Am. Ceram. Soc.* **49**, 404 (1966).
- ⁷⁸E. S. Zouboulis, M. Grimsditch, A. K. Ramdas, and S. Rodriguez, *Phys. Rev. B* **57**, 2889 (1998).
- ⁷⁹W. J. Nellis, J. A. Moriarty, A. C. Mitchell, M. Ross, R. G. Dandrea, N. W. Ashcroft, N. C. Holmes, and G. R. Gather, *Phys. Rev. Lett.* **60**, 1414 (1988).
- ⁸⁰R. G. Greene, H. Luo, and A. L. Ruoff, *Phys. Rev. Lett.* **73**, 2075 (1994).
- ⁸¹N. Nishimura, K. Kinoshita, Y. Akahama, and H. Kawamura, in *Proceedings Joint 20th AIRAPT & 43th EHPRG International Conference on High Pressure Science and Technology*, 27 June–1 July 2005, Karlsruhe Germany (Forschungszentrum Karlsruhe, Karlsruhe, 2005).
- ⁸²J. Hu, H. K. Mao, and P. M. Bell, *High Temp. - High Press.* **16**, 495 (1984).
- ⁸³M. Hanfland, K. Syassen, and J. Köhler, *J. Appl. Phys.* **91**, 4143 (2002).
- ⁸⁴H. Cynn and C. S. Yoo, *Phys. Rev. B* **59**, 8526 (1999).
- ⁸⁵K. Syassen and W. B. Holzapfel, *J. Appl. Phys.* **49**, 4427 (1978).
- ⁸⁶A. Dewaele, P. Loubeyre, and M. Mezouar, unpublished data for Ag.
- ⁸⁷J. C. Jamieson, J. N. Fritz, and M. H. Manghnani, in *High Pressure Research in Geophysics*, edited by S. Akimoto and M. H. Manghnani (Center for Academic Publications, Tokyo, 1982), p. 27.
- ⁸⁸D. L. Heinz and R. Jeanloz, *J. Appl. Phys.* **55**, 885 (1984).
- ⁸⁹K. Takemura, *J. Appl. Phys.* **89**, 662 (2001).
- ⁹⁰T. Yagi, K. Okabe, N. Nishiyama, A. Kubo, and T. Kikegawa, *Phys. Earth Planet. Inter.* **143-144**, 81 (2004).
- ⁹¹N. C. Holmes, J. A. Moriarty, G. R. Gather, and W. J. Nellis, *J. Appl. Phys.* **66**, 2962 (1989).
- ⁹²Y. Fei, J. Li, K. Hirose, W. Minarik, J. Van Orman, C. Sanloup, W. Van Westrenen, T. Komabayashi, and K. Funakoshi, *Phys. Earth Planet. Inter.* **143-144**, 515 (2004).
- ⁹³S. Speziale, C. C. Zha, T. S. Duffy, R. J. Hemley, and H. K. Mao, *J. Geophys. Res.* **106B**, 515 (2001).
- ⁹⁴A. Dewaele, G. Fiquet, D. Andrault, and D. Hausermann, *J. Geophys. Res.* **105B**, 2869 (2000).
- ⁹⁵P. Gillet, G. Fiquet, I. Daniel, and B. Reynard, *Phys. Rev. B* **60**, 14660 (1999).
- ⁹⁶P. I. Dorogokupets and A. R. Oganov (in preparation).
- ⁹⁷R. A. Robie, B. S. Hemingway, and J. R. Fisher, *U. S. Geol. Surv. Bull.* **1452**, 1 (1978).
- ⁹⁸P. I. Dorogokupets and A. R. Oganov, *Dokl. Earth Sci.* **410**, 1091 (2006).
- ⁹⁹Y. Fei, J. Li, K. Hirose, W. Minarik, J. Van Orman, C. Sanloup, W. Van Westrenen, T. Komabayashi, and K. Funakoshi, *Phys. Earth Planet. Inter.* **143-144**, 515 (2004).
- ¹⁰⁰S. Merkel, H. R. Wenk, J. Shu, G. Shen, P. Gillet, H. K. Mao, and R. J. Hemley, *J. Geophys. Res.* **107B**, 2271 (2002).
- ¹⁰¹Y. Akahama, H. Kawamura, and A. K. Singh, *J. Appl. Phys.* **92**, 5892 (2002); **95**, 4767 (2004).
- ¹⁰²M. Matsui and N. Nishiyama, *Geophys. Res. Lett.* **29**, 1368 (2002).
- ¹⁰³N. Nishiyama, T. Irifune, T. Inoue, J. Ando, and K. Funakoshi, *Phys. Earth Planet. Inter.* **143**, 185 (2004).
- ¹⁰⁴Y. Fei, J. Van Orman, J. Li, W. Van Westrenen, C. Sanloup, W. Minarik, K. Hirose, T. Komabayashi, M. Walter, and K. Funakoshi, *J. Geophys. Res.* **109**, B02305 (2004).
- ¹⁰⁵T. Inoue, T. Irifune, Y. Higo, T. Sanehira, J. Ando, K. Funakoshi, and W. Utsumi, *Phys. Chem. Miner.* **33**, 106 (2006).
- ¹⁰⁶K. Hirose, R. Sinmyo, N. Sata, and Y. Ohishi, *Geophys. Res. Lett.* **33**, L01310, doi:10.1029/2005GL024468 (2006).
- ¹⁰⁷T. Tsuchiya, *J. Geophys. Res.* **108**, 2462 (2003).
- ¹⁰⁸O. L. Anderson, D. G. Isaak, and S. Yamamoto, *J. Appl. Phys.* **65**, 1534 (1989).
- ¹⁰⁹P. Souvatzis, A. Delin, and O. Eriksson, *Phys. Rev. B* **73**, 054110 (2006).
- ¹¹⁰C. W. Greff and M. J. Graf, *Phys. Rev. B* **69**, 054107 (2004).
- ¹¹¹A. R. Oganov and S. Ono, *Nature (London)* **430**, 445 (2004); S. Ono, T. Kikegawa, and Y. Ohishi, *Solid State Commun.* **133**, 55 (2005).
- ¹¹²Detailed tables with x - T - P relations are available from the authors.
- ¹¹³N. Mounet and N. Marzari, *Phys. Rev. B* **71**, 205214 (2005).